

Cyclotron Resonance in the Layered Perovskite Superconductor Sr_2RuO_4

S. Hill[†]

Department of Physics, Montana State University, Bozeman, MT 59717

J. S. Brooks

Department of Physics and National High Magnetic Field Laboratory, Florida State University, Tallahassee, FL 32310

Z. Q. Mao and Y. Maeno

Department of Physics, University of Kyoto, Kyoto 606-8502, and CREST-JST, Kawaguchi, Saitama 332-0012, Japan

(May 19, 2019)

We have measured the cyclotron masses in Sr_2RuO_4 through the observation of periodic-orbit-resonances – a magnetic resonance technique closely related to cyclotron resonance. We obtain values for the α , β and γ Fermi surfaces of $(4.33 \pm 0.05)m_e$, $(5.81 \pm 0.03)m_e$ and $(9.71 \pm 0.11)m_e$ respectively. The appreciable differences between these results and those obtained from de Haas-van Alphen measurements are attributable to strong electron-electron interactions in this system. Our findings appear to be consistent with predictions for a strongly interacting Fermi liquid; indeed, semi-quantitative agreement is obtained for the electron pockets β and γ .

PACS numbers: 71.18.+y, 71.27.+a, 74.25.Nf

The perovskite superconductor Sr_2RuO_4 is currently the subject of intense research activity [1]. Initial interest was driven by the structural similarities between this compound and the high- T_c cuprates [2]. However, a clear picture has since emerged in which it apparently belongs to an entirely different class of superconductor. In particular, Sr_2RuO_4 shares many properties with liquid ^3He . For example: the normal state conforms to the behavior expected of a strongly correlated Fermi liquid [3,4]; the highest reported T_c is still relatively low (< 1.5 K); T_c is extremely sensitive to non-magnetic impurities [5]; and there is mounting evidence supporting the view that the superconductivity is induced by ferromagnetic fluctuations, resulting in spin-triplet pairing [6,7].

One of the many attractive features of the title compound has been the availability of high quality single crystals. This has enabled experimental investigations which have not been possible in the high- T_c counterparts, including de Haas - van Alphen (dHvA) and Shubnikov - de Haas (SdH) measurements [3,8]. Consequently, an extensive body of experimental data has given rise to an increasingly coherent picture of the normal state electronic structure [8] which is in broad agreement with the calculated band structure obtained by Local Density Approximations (LDA) [9]. However, as with many strongly correlated electron systems, there is a considerable discrepancy between the calculated and measured density of states at the Fermi energy (E_F); LDA calculations underestimate the effective masses for the three Fermi surface (FS) pockets (two electron and one hole) by factors of between 3 and 5, as determined by dHvA measurements [3]. This difference has been attributed to the Fermi liquid corrections expected in an interacting Fermi system.

The aim of the present study is to measure the cyclotron masses in Sr_2RuO_4 using a long wavelength probe

($Q \sim 0$) which couples to the center-of-mass motion of the system. For an isotropic Fermi liquid, the mass measured in this way corresponds to a different physical quantity than the thermodynamic effective mass m^* [10]; the latter includes enhancements due to the fact that as quasiparticles move through a medium, they experience a drag force resulting from the displacement of other quasiparticles. Thus, in strongly interacting Fermi systems, m^* includes corrections not ordinarily included in band calculations. A cyclotron resonance (CR) experiment, on the other hand, ought to be insensitive to electron-electron interaction (EEI) effects due to the absence of quasiparticle drag in the center-of-mass frame. Therefore, a comparison between the CR mass (hereon denoted m_c) and m^* offers the unique possibility of directly gauging the strength of EEIs. We wish to point out, however, that a CR experiment should be sensitive to other many-body interactions, *e.g.* electron-phonon [10]. Consequently, m_c need not necessarily agree with band calculations.

dHvA experiments on Sr_2RuO_4 have confirmed the existence of three quasi-two-dimensional (cylindrical) FSs whose cross sections are weakly modulated (warped) along the c -direction [3,8]. Application of a magnetic field causes carriers to orbit these roughly cylindrical FSs in a plane perpendicular to the field. The dominant result is cyclotron motion within the conducting layers, even when the field is tilted well away from the c -axis. It is this cyclotron motion that one usually couples to in a CR experiment. However, this is not the approach that we follow. A more subtle effect concerns the influence of a magnetic field on the carrier velocities parallel to the cylinder axes. Depending on the field orientation, and on the symmetry of the warping, the c -axis velocities (v_c) will also oscillate (for a detailed discussion, see ref

[11]). This has resulted in the prediction of a new kind of CR, the so-called "Periodic Orbit Resonance" (POR) [11], which involves coupling resonantly to these periodic modulations of v_c . The fundamental frequencies are, of course, the classical cyclotron frequencies. However, one can additionally expect to observe harmonics due to the non trivial way in which the periodic reciprocal space orbits translate into v_c modulations [11,12]. POR have since been observed in several low-dimensional organic conductors [13,14].

The POR technique offers a major advantage over conventional CR in the case of Sr_2RuO_4 , where the high *ab*-plane conductivity makes it extremely difficult to observe the latter effect [15]. At 1.5 K and 50 GHz, we estimate an *ab*-plane penetration depth of $\delta \approx 0.2 \mu\text{m}$. This compares with a mean free path of $\lambda \approx 1 \mu\text{m}$ and cyclotron radii at resonance of no greater than $r_c = 0.5 \mu\text{m}$ – this is the anomalous skin effect regime. Although it should be possible to detect bulk CR under these conditions, through the influence of the bulk *ab*-plane conductivity on the surface impedance of the sample, we anticipate an extremely weak signal with a very broad distorted line-shape (this is discussed at length in refs. [11,15]). Furthermore, we can rule out the possibility of observing Azbel'-Kaner CR, which requires $r_c/\delta \gg \sqrt{\omega\tau}$ [11]. In contrast, a measurement of the *c*-axis conductivity will not suffer from these problems.

Because of the large effective masses in Sr_2RuO_4 , it was necessary to conduct experiments at the lowest frequencies allowed by the constraint $\omega\tau > 1$, and to use high magnetic fields. The high quality of the Sr_2RuO_4 single crystal used in this study, which was grown by a floating zone method [4] and has a T_c of 1.44 K (mid-point), enabled measurements in the mm-wave spectral range. One of the benefits of working at these low frequencies is the possibility of utilizing an extremely sensitive cavity perturbation technique [16]. Fields of up to 33 tesla were provided by the resistive magnets at the National High Magnetic Field Laboratory in Florida.

Two different cylindrical copper cavities ($\phi \sim 10\text{mm}$, height $\sim 10\text{mm}$) were used in transmission, providing four $\text{TE}01n$ ($n = 1, 2$ and 3) modes in the desired frequency range. A single Sr_2RuO_4 crystal (dimensions $\approx 2 \times 1 \times 0.2\text{mm}^3$) was placed close to the bottom of the cavity, half way between its axis and its perimeter, thereby ensuring that the sample was optimally coupled to the radial AC magnetic fields (\mathbf{B}_1) for a given $\text{TE}01n$ mode. The sample *c*-axis was aligned with the cavity axis and, therefore, parallel to the applied DC magnetic field (\mathbf{B}_o), i.e. $\mathbf{B}_1 \perp \mathbf{B}_o$. In this configuration ($\mathbf{B}_1 // ab\text{-plane}$), it is expected that the microwave fields will penetrate the bulk of the sample, and that dissipation will be dominated by the *c*-axis conductivity due to the excitation of inter-layer currents [16], *i.e.* this configuration is ideal for observing POR [13,14]. Loaded cavity *Q*-factors ranged from 5×10^3 to 2×10^4 depending on the mode and on

the orientation of the sample within the cavity. As a spectrometer, we used a Millimeter-wave Vector Network Analyzer (MVNA) [16]. The cavity and, therefore, the sample could accurately and controllably be maintained at any temperature between 1.4 K and 30 K.

Fig. 1a shows changes in the absorption within the cavity as a function of magnetic field for several temperatures in the range 1.4 to 6 K [17]. The cavity was excited at 76.4 GHz, which corresponds to its $\text{TE}013$ mode. The data were obtained after subtracting a background cavity response and have been offset for the sake of clarity. It is apparent that on cooling below ~ 5 K, a series of absorption peaks develop and grow stronger. The peak positions appear to be independent of temperature, as illustrated by the Lorentzian fits to the data. The number of Lorentzians, and the initial estimates of their peak positions, were chosen after inspecting data obtained at four different frequencies (see Fig. 3). Otherwise, all parameters in the fitting procedure were free running. Fig. 1b shows an almost identical data set obtained at a lower frequency of 64.0 GHz, which corresponds to the $\text{TE}013$ mode of the second cavity. It should be noted that all of the absorption peaks have shifted to lower magnetic field.

Similar data were obtained at 44.5 GHz and 58.5 GHz, corresponding to the $\text{TE}011$ and $\text{TE}012$ modes of the first cavity respectively. However, the absorption peaks were less clearly resolved from each other at these lower frequencies due to the lower $\omega\tau$ product. In the inset to Fig. 2, we show a magnified portion of the high field 44.5 GHz data (highest *Q* mode); SdH oscillations are clearly visible. A fourier transform gives rise to a single peak (main part of Fig. 2) at a frequency of 2975 T, in good agreement with the α -frequency reported previously [3]. Thus, we can be extremely confident that we are well coupled to the sample within the cavity. Weaker SdH oscillations (due to lower *Q*-values) were discernible in all but the highest frequency data. The absence of β and γ frequencies in the SdH spectra is due to the relatively high temperature (1.4 K) of these measurements.

Fig. 3 shows a compilation of the absorption peak-field positions plotted against frequency for the four $\text{TE}01n$ cavity modes used in this study. The exact peak-field positions were obtained from fits to 1.4 K data. All of the points fall nicely on one of several straight lines which pass through the origin, as expected for cyclotron-like resonances.

Because of the experimental configuration, we assume that the additional absorption within the cavity results from the resonant excitation of currents in the least conducting direction within the sample. Consequently, we attribute the absorption peaks seen in Fig. 1 to the POR phenomena discussed above and in refs [11,12,13,14]. Several features of the data provide strong backing for this interpretation. To begin with, the scaling of the

resonance peak-field positions with frequency (Fig. 3) confirms that cyclotron motion is indeed responsible this effect. Meanwhile, the Lorentzian lineshapes indicate that it is the real part of the c -axis conductivity which is directly responsible for dissipation in the cavity, rather than the ab -plane surface resistance (see refs. [11,15]).

Although four dominant resonances are seen in Fig. 3 (in fact, there are more - see inset to Fig. 3), we can account for all of the data in terms of three independent carrier types. The inset to Fig. 3 shows an enlarged view of the low field (high $1/\mathbf{B}$) portion of the $f = 76.4$ GHz data plotted versus ω/ω_c , where $\omega = 2\pi f$ and ω_c is the cyclotron frequency ($e\mathbf{B}/m_c$). The resonances labeled $N=1$ and $N=2$ correspond respectively to the up (Δ) and down (∇) triangle data points in the main part of the figure. It is apparent that the $N=1$ peak is actually the first in a harmonic series with resonances visible up to $N=4$. Thus, we attribute all of these peaks to a single FS. Further confirmation of this can be found from fits to the data in the main part of Fig. 3 where the slopes obtained for the up and down triangle data points differ by a factor of exactly 2 (± 0.04).

The remaining resonances are not related harmonically, either to each other, or to the data in the inset to Fig. 3. Thus, we conclude that the POR response is attributable to three independent carrier types – in agreement with both the theoretically [9] and experimentally determined FS [8]. We assign the heaviest POR mass $m_{c\gamma} = (9.71 \pm 0.11)m_e$ to the γ -FS which, to our knowledge, is the largest electronic effective mass thus far detected by magnetic resonance. The POR mass for the β -FS is $m_{c\beta} = (5.81 \pm 0.03)m_e$, while we attribute the harmonic series of PORs to the α -FS with a mass $m_{c\alpha} = (4.33 \pm 0.05)m_e$.

Before addressing the obvious differences between the masses obtained from these studies and those deduced by Mackenzie *et al.* [8], several features of the data deserve further discussion. To begin with, it is perhaps surprising that POR are observed at all when the magnetic field is applied parallel to the c -axis, *i.e.* parallel to the induced AC currents. Classically, one does not expect a magnetic field to influence motion along an axis parallel to itself, because there is no Lorentz force in this direction. However, it is possible to envisage a warped FS in which the velocities (not momenta) in this direction do oscillate [11]. This scenario is also consistent with the observation of a finite c -axis longitudinal magnetoresistance [18]. Further angle dependent POR investigations should be able to determine the exact symmetry of the warping and, therefore, reveal important information about the inter-layer conduction mechanism [11].

Next we turn our attention to the fact that the α PORs have a strong high harmonic content, whereas there is no clear evidence of this for the other two resonances. A plausible explanation can be found by examining the predicted FS [9]. The two electron-like pockets, β and

γ , have almost circular cross sections. In contrast, the hole pocket has more of a diamond shaped cross section, as has recently been confirmed experimentally [19]. Consequently, the observation of POR harmonics is a clear manifestation of the lower symmetry of this FS [12].

A comparison between the cyclotron masses deduced in this study and the thermodynamic masses ($m_\alpha^* = 3.4m_e$, $m_\beta^* = 7.5m_e$ and $m_\gamma^* = 14.6m_e$) measured by Mackenzie *et al.* [8], reveal clear enhancements of m^* over m_c for the electron-like FSs (β and γ). This does not appear to be the case for the hole-like (α -) FS. However, in a recent study by Yoshida *et al.* [20], it is claimed that the dHvA mass for the α -pocket is $m_\alpha^* = 4.3m_e$. This larger value is a little more consistent with the α -POR mass deduced in this study.

According to Fermi liquid theory, the ratio between m^* and the so-called dynamical mass which, in this case, we are assuming corresponds to the cyclotron mass m_c , is given by $m^*/m_c = 1 + F_1^s/3$, where F_1^s is the dimensionless $l = 1$ Fermi liquid parameter [10]. In turn, F_1^s should be proportional to the thermodynamic density of states at E_F which, for a two-dimensional system, is proportional to the thermodynamic effective mass at E_F , *i.e.* $F_1^s \propto m^*$. Consequently, one expects the mass enhancements $[(m^*/m_c) - 1]$ to scale with the thermodynamic masses m^* . Interestingly, a comparison between our results and the dHvA masses reported by Mackenzie *et al.* [8], reveal that the mass enhancements for the β and γ FSs scale most closely with the cyclotron masses $m_{c\beta}$ and $m_{c\gamma}$, *i.e.* $[(m_\gamma^*/m_{c\gamma}) - 1]/[(m_\beta^*/m_{c\beta}) - 1] = 1.73$ and $m_{c\gamma}/m_{c\beta} = 1.67$. Nevertheless, the thermodynamic mass ratio ($m_\gamma^*/m_\beta^* = 1.95$) is not too far off from 1.73 either. Indeed, if one uses the β dHvA mass ($7.2m_e$) from ref. [20] and the γ dHvA mass from ref. [8], the mass enhancement ratio and the thermodynamic mass ratio both come out close to 2. All said and done, the very fact that the β and γ mass enhancements seem to scale with the effective masses lends strong support to the assertion that Sr_2RuO_4 is a strongly correlated Fermi liquid.

A word of caution is appropriate at this point. The underlying theory used in the above analysis was developed for a single-band isotropic Fermi liquid. In Sr_2RuO_4 , one might expect a strong coupling between the various cyclotron modes corresponding to each electron or hole band. In turn, these couplings might be expected to have a pronounced effect on the measured cyclotron frequencies, over and above the effects expected for a simple Fermi liquid. With this in mind, it is reasonable to expect the dominant electronic modes (β and γ) to have more of an influence on the hole mode (α) [21], as opposed to the other way round, which might explain why the α -data do not follow the same trends seen for the β and γ FSs. We note in passing that the ratios, m_c/m_b , between the measured cyclotron masses and the calculated band masses are quite similar for the β ($m_{b\beta} =$

$2m_e$) and γ ($m_{b\gamma} = 2.9m_e$) FSs, while this is not the case for the α pocket ($m_{b\alpha} = 1.1m_e$).

Finally, we consider the temperature dependence of the PORs, which attenuate dramatically above 3 K. This is not expected for a single non-interacting parabolic band, unless the quasiparticle lifetime τ depends strongly on temperature. One explanation, therefore, is that the T^2 dependence of $1/\tau$ is responsible for this attenuation [4]. However, we cannot rule out the possibility that above ~ 3 K, when $k_B T$ exceeds $\hbar\omega_c$, the POR lines broaden due to non-parabolicity. Interactions would then further attenuate the resonances due to the broadened distribution of cyclotron frequencies.

In summary, we have measured the cyclotron masses corresponding to the α , β and γ FSs in Sr_2RuO_4 . Comparisons between these values and those deduced from dHvA studies reveal considerable enhancements of the thermodynamic effective masses which we attribute to strong electron-electron interactions. Qualitatively, our findings are in good agreement with Fermi liquid theory.

This work was supported by the Office of Naval Research. Work carried out at the NHMFL was supported by a cooperative agreement between the State of Florida and the NSF under DMR-95-27035.

[†] email: hill@physics.montana.edu

- [1] Y. Maeno, *Physica C* **282-287**, 206 (1997), and references therein.
- [2] Y. Maeno *et al.*, *Nature* **372**, 532 (1994).
- [3] A. P. Mackenzie *et al.*, *Phys. Rev. Lett.* **76**, 3786 (1996).
- [4] Y. Maeno *et al.*, *J. Phys. Soc. Jpn* **66**, 1405 (1997).
- [5] A. P. Mackenzie *et al.*, *Phys. Rev. Lett.* **80**, 161 (1998).
- [6] T. M. Rice *et al.*, *J. Phys. Cond. Matt.* **7**, L643 (1995).
- [7] K. Ishida *et al.*, *Nature* **396**, 658 (1998).
- [8] See discussion in: A. P. Mackenzie *et al.*, *J. Phys. Soc. Jpn* **67**, 385 (1998), and references therein.
- [9] T. Oguchi, *Phys. Rev. B* **51**, 1385 (1995); and D. J. Singh, *Phys. Rev. B* **52**, 1358 (1995).
- [10] K. F. Quader *et al.*, *Phys. Rev. B* **36**, 156 (1987), and references therein.
- [11] S. Hill, *Phys. Rev. B* **55**, 4931 (1997).
- [12] S. J. Blundell *et al.*, *Phys. Rev. B* **55**, 6129 (1997).
- [13] A. Ardavan *et al.*, *Phys. Rev. Lett.* **81**, 713 (1998).
- [14] S. Hill *et al.*, in preparation.
- [15] S. Hill *et al.*, *Phys. Rev. B* **54**, 13536 (1996).
- [16] S. Hill *et al.*, *Physica B* **246-247**, 110 (1998), and references therein.
- [17] A detailed description of how the absorption is measured in our experiments is given in ref. [16].
- [18] N. E. Hussey *et al.*, *Phys. Rev. B* **57**, 5505 (1998).
- [19] E. Omichi *et al.*, *Phys. Rev. B* **59**, 7263 (1999).
- [20] K. Yoshida *et al.*, *J. Phys. Soc. Jpn* **67**, 1677 (1998).
- [21] One might expect the strongest interaction to occur between α and β which share the same dominant d_{yz} and d_{zx} character.

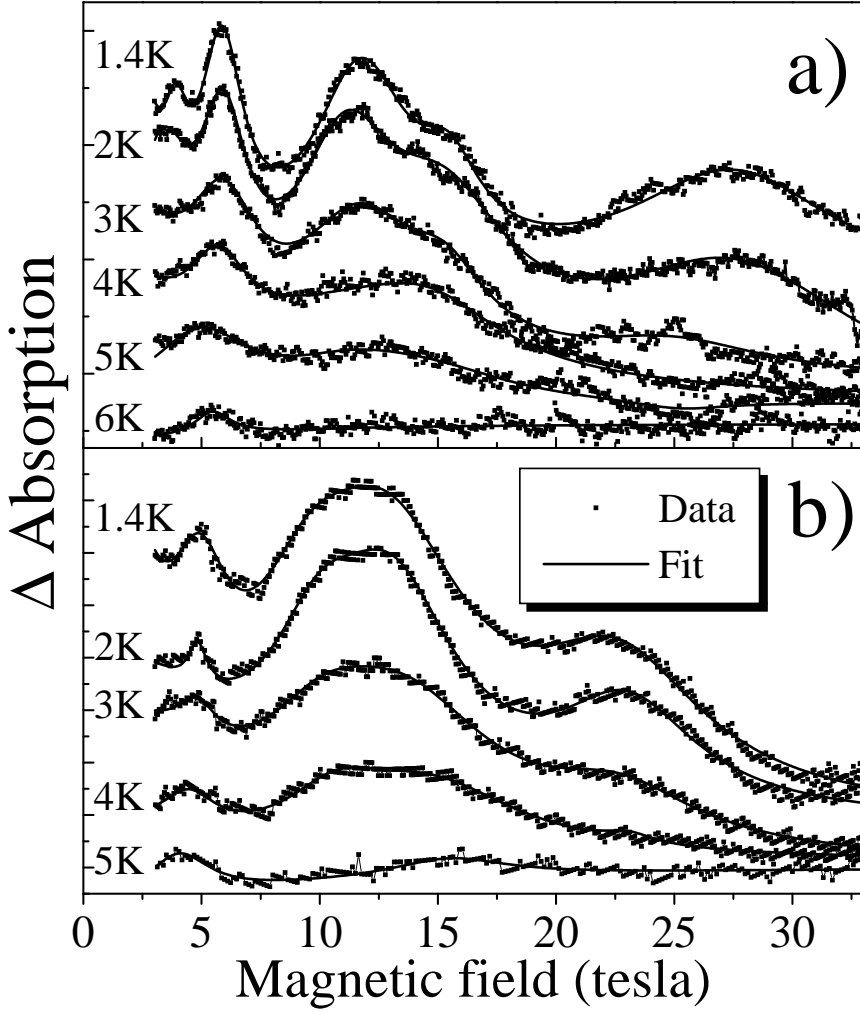


FIG. 1. Temperature and magnetic field dependence of the changes in absorption within the cavity (after a background subtraction) at a) 76.4 GHz, and b) 64 GHz; the data have been offset for the sake of clarity. See text for an explanation of the fitting procedure.

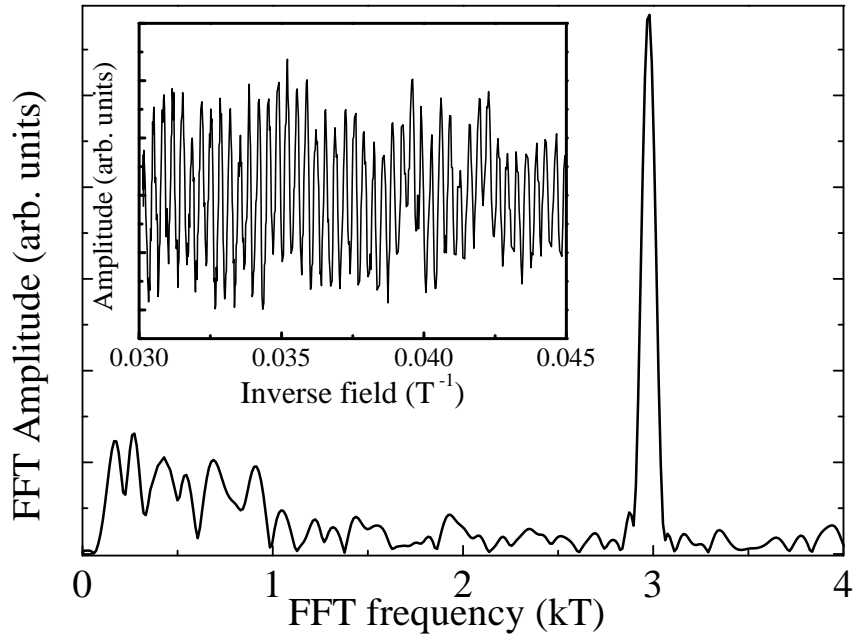


FIG. 2. Fast fourier transform (FFT) of the high-field cavity response (inset) at 44.5 GHz and at 1.4 K. SdH oscillations are visible in the inset which are periodic in $1/\mathbf{B}$. These oscillations correspond to the α -frequency observed in ref. [3].

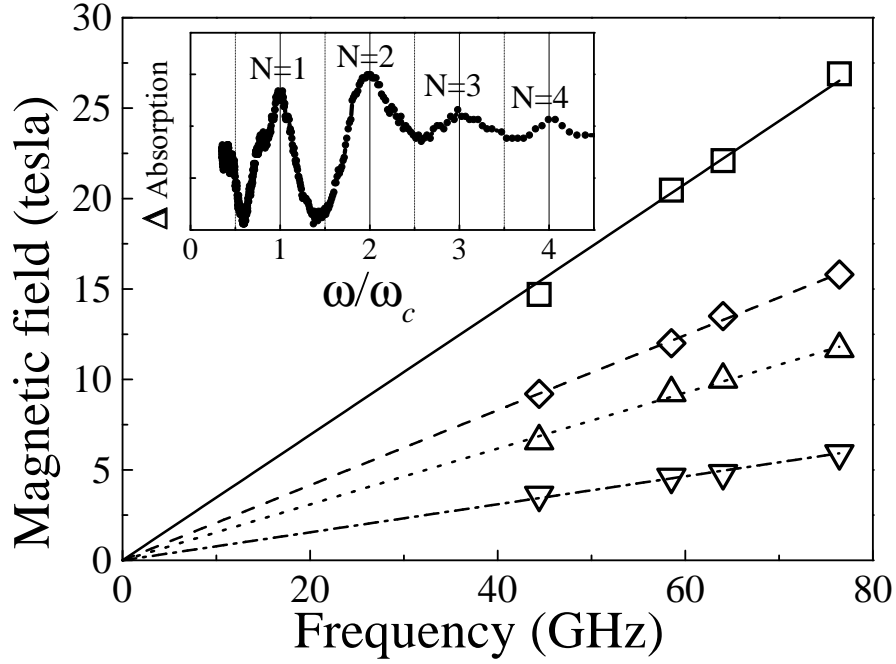


FIG. 3. Plots of the POR peak-field positions versus frequency at 1.4 K. We assign the resonances as follows: $\square - \gamma$, $\diamond - \beta$, $\triangle - \alpha$ 1st harmonic, and $\nabla - \alpha$ 2nd harmonic. The inset shows the α -series of POR harmonics at 76.4 GHz, plotted versus inverse field.